Available online at www.sciencedirect.com
SCIENCE DIRECT®
European Journal of Mechanics B/Fluids 24 (2005) 586–595

Interactions between hard spheres sedimenting at low Reynolds number

Claude Vanroyen [a,*], Abdelaziz Omari [b], Jean Toutain [a], David Reungoat [a]

[a] *Laboratoire de Transferts, Ecoulements, Fluides, Energétique (UMR 8508) ENSCPB, 16, av. Pey Berland, BP 108-33607, Pessac cedex France*

[b] *Laboratoire des Milieux Dispersés Alimentaires, ISTAB, av. des facultés, 33405 Talence cedex France*

Received 9 September 2004; received in revised form 19 November 2004; accepted 10 January 2005

Available online 8 February 2005

Abstract

The present article reports on experimental and numerical study for sedimentation of non-colloidal suspended particles in a viscous fluid. The hydrodynamic interactions between several particles sedimenting at low Reynolds numbers have been investigated. The numerical model is based on separation of the real velocity field into two parts. The first part is symmetrical and represents the conventional Stokes contribution. The second non-symmetrical part represents the net inertial contribution. The first contribution has been modelled using the Stokesian Dynamics method. Whereas the second one has been accounted for by assuming the validity of Faxen's first law. The numerical results agree with those from literature in the limit of the Stokes' flow regime ($Re = 0$). Unfortunately, when $Re > 0$, the simulation appears to quantitatively overestimate the influence of the real inertial effects. However, the accuracy of the results has been observed to be improved by introducing the empirical correction proposed by Happel et al. at the level of the individual particle. In this way, the proposed numerical tool becomes able to determine accurately the behaviour of several particles in different configurations. The agreement between the simulation results and the experimental ones is very satisfactory.
© 2005 Elsevier SAS. All rights reserved.

Keywords: Sedimentation; Hydrodynamic interactions; Inertial effects; Simulation; Experiment

1. Introduction

Fluid flow involving suspensions of solid particles finds applications in many industrial processes. These suspensions when flowing involve various interactions since the particles are subjected to forces of diverse causes. Concerning colloidal suspensions (micronic and sub-micronic particles), gravitational forces may be neglected when compared to the other forces acting on the particles. The rheology of such a suspension also depends on the hydrodynamic interactions, on the disjoining pressure as well as on diffusion. When the size of the particles becomes millimetric, the suspension's behaviour is mostly governed by the hydrodynamic interaction forces and the gravitational forces. Moreover, when the particle-wall distances decrease, the influence of the confinement produces undesirable effects such as non-homogeneous concentration profiles.

* Corresponding author. Tel.: +(33) 5 40 00 28 76; fax: +(33) 5 56 37 03 36.
E-mail address: vanroyen@enscpb.fr (C. Vanroyen).

0997-7546/$ – see front matter © 2005 Elsevier SAS. All rights reserved.
doi:10.1016/j.euromechflu.2005.01.002

For low values of particles volume fraction, taking the two-body hydrodynamic interactions into consideration has been found to be sufficient to correctly describe the system. However, for higher volume fraction, it is therefore necessary to consider the multi-body interactions [1]. On the other hand, the near field interaction forces (lubrication) may play a predominant role when the surface-to-surface distance becomes too low [2].

If the flow is creeping, the inertial effects can be ignored and the suspension's behaviour as a whole can be deduced from hydrodynamic interactions in Stokes' flow regime (i.e. $Re = 0$). However, the dispersed particles are generally transported at a velocity such that the Reynolds number is actually nonzero. Thus, the flow cannot be considered as creeping and the momentum equation of the fluid phase is non-linear.

Analytical expressions of the particle hydrodynamic interaction forces are available only in Stokes' flow regime. For values of the Reynolds number in the order of $Re \simeq 0.1$, direct calculation of these interactions can be carried out numerically, for example by applying a reflection method to the velocity fields generated by each particle on the remaining ones [3]. However, this method is laborious and expensive and its application is restricted to large center-to-center distances and to low number of particles. These difficulties explain why numerical models dealing with the flow of undiluted suspensions in inertial regimes are rare.

The aim of the present work is to propose an alternative numerical approach allowing to consider this kind of flow at reasonable computational cost. The usual formulation in Stokes conditions is partially retrieved when the inertial effects are introduced writing the actual velocity field as that of two contributions: a Stokesian part and an inertial part. The propagation of the Stokesian part is calculated using the previously approach proposed by Durlofsky et al. [1], while the propagation of the inertial part is expressed explicitly in terms of relative fluid-particle velocity.

The present article is organised as follows. The details of the model and the methodology used are presented in Section 2. Experiments on the sedimentation of particles at low Reynolds number were also performed using the techniques and the methods that are described in Section 3. The numerical results, their comparison with experimental data and the discussion are presented in Section 4.

2. Numerical model

2.1. Theoretical considerations

The description of hydrodynamic interactions within a suspension consists of determining the velocity $\mathbf{U}$ of the particles, knowing the forces $\mathbf{F}$ to which they are subjected. The relation between $\mathbf{U}$ and $\mathbf{F}$ can be written as $\mathbf{U} = \mathbf{M}\mathbf{F}$, where $\mathbf{M}$ is the mobility matrix [1,4,5]. Alternatively, the problem can be formulated in terms of resistance matrix $\mathbf{R}$ [6–9]. The forces applied to each particle are determined using: $\mathbf{F} = \mathbf{R}\mathbf{U}$. The elements of the mobility matrix $\mathbf{M}$ or the resistance matrix $\mathbf{R}$, are tensors which express the interactions between two particles along and perpendicular to their center-to-center vector.

Within a suspension, the hydrodynamic force $\mathbf{F}$ is the sum of a far field contribution $\mathbf{F}^{\text{far}}$ and a near field contribution (lubrication) $\mathbf{F}^{\text{lub}}$: $\mathbf{F} = \mathbf{F}^{\text{far}} + \mathbf{F}^{\text{lub}}$. It is then possible in principle to describe the behaviour of non-homogeneous suspensions containing zones of low concentration, where the far field interaction forces prevail, and containing high-concentration zones where close field interaction forces are predominant [1,10].

Under Stokes conditions, both tensors elements of matrix $\mathbf{M}$ and $\mathbf{R}$ may be calculated [1,8,9] for two interacting spheres. When several particles are considered, calculation of their hydrodynamic interactions needs to take into account the multi-body contribution. For that purpose, Durlofsky et al. [1] have proposed a simple way to determine the tensors elements of $\mathbf{R}$.

Even in inertial regime, tensors elements of $\mathbf{R}$ may be calculated for two interacting spheres in the limit of $Re \ll 1$ [11,12]. However, calculation of multi-body interactions have not been considered. In the present study, an alternative approach is developed as explained in the following sections.

2.2. Hydrodynamic forces

2.2.1. Far field contribution

The inertial forces originate from the fluid motion as it is produced by the particle displacement. For a particle with a uniform velocity $\mathbf{U}$, suspended in an infinite Newtonian fluid initially at rest, the momentum equation reduces, for low Reynolds numbers, to the well known Oseen equation [13]:

$$\begin{aligned} -(\mathbf{U}\cdot\nabla)\mathbf{v} &= -\frac{1}{\rho}\nabla p + \frac{\mu}{\rho}\Delta\mathbf{v}, \\ \nabla\cdot\mathbf{v} &= 0 \end{aligned} \tag{1}$$

where $\mathbf{v}$ is the fluid velocity and where ρ and p stand for the density of the incompressible fluid and the pressure respectively. The velocity field deduced from Eq. (1) is usually given in terms of the stream function ψ expressed in spherical coordinates (R, θ) as:

$$\psi = Ua^2\left[-\frac{a}{4R}\sin^2\theta + 3(1+\cos\theta)\frac{1-\exp(-(1/4)Re(1-\cos\theta)R/a)}{Re}\right]. \tag{2}$$

This approximate solution to O(Re) is consistent with the degree of approximation used to obtain Eq. (1). As pointed out by Batchelor [13], in the close vicinity of the sphere and at very low Reynolds number Eq. (2) coincides with Stokes's solution with a relative error of order Re. At larger distance from the sphere, the velocity field given by Eq. (2) represents the actual velocity field as accurately as the needed order of approximation.

On contrary to the case of zero Reynolds number, the Oseen velocity field shows an up-and-downstream asymmetry. Such asymmetry explains the typical behaviour of interacting spheres in inertial flow. For an isolated sphere at low Reynolds number, the drag force $\mathbf{F}$ is theoretically a linear function of Re:

$$\mathbf{F} = -6\pi\mu a\mathbf{U}\left(1+\frac{3}{16}Re\right). \tag{3}$$

Calculation of the hydrodynamic interaction forces between particles can be carried out numerically using a reflection technique applied to Oseen velocity fields generated by each particle [3]. However, accurate numerical calculation of hydrodynamic interactions by means of reflection method is computationally expensive, not only when the particles are close [14], but also when several particles interact. For these reasons, this technique is restricted to cases of low number of particles and to configurations where distances between particles are not too small.

In the present work, we propose an alternative method, analogous to that proposed by Durlofsky et al. [1], in order to consider the hydrodynamic interactions with inertial effects at small Reynolds number. This method consists of formally separating the velocity field generated by particles in inertial regime, into a purely Stokesian part and a non-Stokesian contribution. Then, the hydrodynamic interaction forces can be calculated assuming the first Faxen law to be still valid. These forces can be introduced into equations arising from Newton's Second Law (NSL) and give access to the velocities and trajectories of the particles.

Considering two identical hard spheres labelled 1 and 2 and subjected to the forces $\mathbf{F}_1$ and $\mathbf{F}_2$ respectively. Their interaction in terms of velocity yields for sphere 1 the following equation:

$$\mathbf{U}_1 = \frac{\mathbf{F}_1}{6\pi\mu a(1+(3/16)Re_1)} + \left(1+\frac{a^2}{6}\nabla^2\right)\mathbf{v}_2^{\mathrm{O}}(\mathbf{x})\Big|_{x=x_1} \tag{4}$$

where $\mathbf{F}_1/(6\pi\mu a(1+\frac{3}{16}Re_1))$ is the instantaneous velocity of sphere 1 and $\mathbf{v}_2^{\mathrm{O}}(\mathbf{x})|_{x=x_1}$ represents the perturbation due to the displacement of particle 2, expressed at the center of sphere 1. Writing $\mathbf{v}_2^{\mathrm{O}}$ as $(\mathbf{v}_2^{\mathrm{S}} + (\mathbf{v}_2^{\mathrm{O}} - \mathbf{v}_2^{\mathrm{S}}))$, where $\mathbf{v}_2^{\mathrm{S}}$ is the Stokesian part of the velocity field, we can express $\mathbf{U}_1$ as:

$$\mathbf{U}_1 = \mathbf{W}_{11}^*\frac{\mathbf{F}_1}{6\pi\mu a(1+(3/16)Re_1)} + \mathbf{W}_{12}^*\frac{\mathbf{F}_2}{6\pi\mu a(1+(3/16)Re_2)} + \left(1+\frac{a^2}{6}\nabla^2\right)\left(\mathbf{v}_2^{\mathrm{O}}(\mathbf{x}) - \mathbf{v}_2^{\mathrm{S}}(\mathbf{x})\right)\Big|_{x=x_1} \tag{5}$$

where tensors $\mathbf{W}_{ij} = \frac{1}{6\pi\mu a}\mathbf{W}_{ij}^*$ are given by:

$$\mathbf{W}_{ij} = \frac{1}{6\pi\mu a}\left[A_{ij}\frac{\mathbf{r}\otimes\mathbf{r}}{r^2} + B_{ij}\left(\delta_{ij} - \frac{\mathbf{r}\otimes\mathbf{r}}{r^2}\right)\right] \tag{6}$$

where $\mathbf{r}$ is the center-to-center vector, $r = \|\mathbf{r}\|$ and $A_{11} = B_{11} = 1$, $A_{12} = (3a)/(2r) - a^3/r^3$ and $B_{12} = 3a/(4r) + a^3/(2r^3)$.

In Eq. (4), hereabove we assumed that the first Faxen law remains valid in low Reynolds number limit. Such assumption is adopted here with respect to the low importance of the Faxen term applied to the non-Stokesian par of velocity field.

After some algebraic calculation, the velocity of each particle may be expressed as follows:

$$\mathbf{U}_i = \left[\sum_{j=1}^{2}\mathbf{W}_{ij}^*\frac{\mathbf{F}_j}{6\pi\mu a}\right] - \left[\frac{3}{16}\sum_{j=1}^{2}\left(Re_j\mathbf{W}_{ij}^*\frac{\mathbf{F}_j}{6\pi\mu a(1+(3/16)Re_j)}\right) - \boldsymbol{\nu}_i\right] \tag{7}$$

where $\boldsymbol{\nu}_i = (1+\frac{a^2}{6}\nabla^2)(\mathbf{v}_j^{\mathrm{O}}(\mathbf{x}) - \mathbf{v}_j^{\mathrm{S}}(\mathbf{x}))|_{x=x_1}$.

For spheres 1 and 2, Eq. (7) may be rewritten in a matrix form as follows:

$$\mathbf{M}\cdot\mathbf{F} = \begin{pmatrix}\mathbf{W}_{11} & \mathbf{W}_{12}\\ \mathbf{W}_{22} & \mathbf{W}_{21}\end{pmatrix}\begin{pmatrix}\mathbf{F}_1\\ \mathbf{F}_2\end{pmatrix} = \left[\mathbf{I} + \frac{3}{16}\begin{pmatrix}Re_1\mathbf{W}_{11}^* & Re_2\mathbf{W}_{12}^*\\ Re_1\mathbf{W}_{21}^* & Re_2\mathbf{W}_{22}^*\end{pmatrix}\right]\begin{pmatrix}\mathbf{U}_1\\ \mathbf{U}_2\end{pmatrix} - \begin{pmatrix}\boldsymbol{\nu}_1\\ \boldsymbol{\nu}_2\end{pmatrix}. \tag{8}$$

Inversion of Eq. (8) provides then the quasi-static contribution of hydrodynamic forces acting on each particle by knowing the instantaneous velocities of all of them. It is to be noticed that if we consider a collection of several interacting spheres, one obtains an similar equation. Inversion of such equation is known to take into account the multi-body effects within the suspension [1].

2.2.2. Near field contribution

A method to calculate the near field interaction forces is to consider only the spheres present in the immediate environment of each sphere. For a given particle these forces are considered nonzero within an interaction perimeter whose dimension is generally of two radius from the center. They are then calculated using equations from lubrication theory, usually used in literature [2,10]. Within the interaction perimeter, lubrication forces are proportional to the relative particle–particle velocity $\mathbf{V}_{ij}$ and depend on the surface-to-surface dimensionless distance ϵ: $\epsilon = (r - 2a)/a = (r^* - 2)$.

The dimensionless forces exerted along and perpendicular to the center-to-center vector $\mathbf{r}$ are respectively given by:

$$\mathbf{f}^{\parallel} = \frac{\mathbf{F}^{\parallel}}{6\pi\mu a\|\mathbf{V}_{ij}\|} = -\frac{1}{4\epsilon} - 0.225\ln\left(\frac{1}{\epsilon}\right) - \frac{3\epsilon}{112}\ln\left(\frac{1}{\epsilon}\right), \tag{9}$$

$$\mathbf{f}^{\perp} = \frac{\mathbf{F}^{\perp}}{6\pi\mu a\|\mathbf{V}_{ij}\|} = \frac{1}{6}\ln\left(\frac{1}{\epsilon}\right). \tag{10}$$

In the present study, the rotation torque due to the velocity gradient when two particles move perpendicularly to $\mathbf{r}$ is ignored. This method will be implemented to calculate the lubrification forces in simulations of sedimenting particles.

2.3. Numerical method

2.3.1. Basic equations

In this part we will present the method to calculate the velocity $\mathbf{U}_i$ and the positions $\mathbf{X}_i$ of n identical spheres of density ρ_p, in sedimentation in a Newtonian viscous fluid of density ρ initially at rest. This calculation consists of solving equations arising from the NSL, at the center of each particle of the system. The added mass forces; $\mathbf{F}^{\mathrm{M}}$; as gravitational body forces; $\mathbf{F}^{\mathrm{V}}$; (weight and upthrust buoyancy) as the hydrodynamic interaction forces; $\mathbf{F}$; are taken into account while the Basset forces are neglected. The Basset force represents the delay effect in settling the fluid motion. Its actual value depends on all past acceleration and may be determined from recording of evolution of particle velocity in course of time [15]. Since for low *Re* and short simulation time, such force should have a small effect, it has been ignored in the present study [14].

So, the equations that we have to solve for each particle are the following:

$$\begin{aligned} m\frac{\mathrm{d}\mathbf{U}_i}{\mathrm{d}t} &= \mathbf{F}_i^{\mathrm{V}} + \mathbf{F}_i^{\mathrm{M}} + \mathbf{F}_i, \\ \frac{\mathrm{d}\mathbf{X}_i}{\mathrm{d}t} &= \mathbf{U}_i \end{aligned} \tag{11}$$

where $\mathbf{F}_i^{\mathrm{V}}$ is always of the form: $\mathbf{F}_i^{\mathrm{V}} = \frac{4}{3}\pi a^3\Delta\rho\mathbf{g}$; with $\Delta\rho = \rho_p - \rho$ and $\mathbf{F}_i^{\mathrm{M}} = -\frac{2}{3}\pi a^3\rho\,\mathrm{d}\mathbf{U}_i/\mathrm{d}t$, while $\mathbf{F}$ depends on the number of particles, on their relative positions and on the instantaneous Reynolds number. The lubrication forces for each particle doublet are calculated by using Eqs. (9) and (10). The far field interaction forces are obtained after inverting Eq. (8), in order to include the multi-body interactions between particles [1] and thus the following form of $\mathbf{F}$ is obtained:

$$\mathbf{F} = -\mathbf{M}^{-1}\cdot\left(\left[\mathbf{I} + \frac{3}{16}\mathbf{Z}\right]\mathbf{U} - \boldsymbol{\nu}\right) + \mathbf{F}^{\mathrm{lub}}. \tag{12}$$

In these conditions, Eq. (11) is rewritten as:

$$\begin{aligned} \frac{\mathrm{d}\mathbf{u}_i}{\mathrm{d}t'} &= \mathbf{u}_i^0 + \mathbf{f}_i, \\ \frac{\mathrm{d}\mathbf{x}_i}{\mathrm{d}t'} &= \frac{\tau U_S}{a}\mathbf{u}_i \end{aligned} \tag{13}$$

with

$$\mathbf{x} = \frac{\mathbf{X}}{z}, \quad \mathbf{u} = \frac{\mathbf{U}}{U_S}, \quad t' = \frac{t}{\tau}, \quad \mathbf{f} = \frac{\mathbf{F}}{6\pi\mu a U_S}, \quad \mathbf{u}_i^0 = (0, -1)$$

where U_S and $\tau = \frac{4}{3}\pi a^3(\rho_p + \frac{1}{2}\rho_f)/(6\pi\mu a)$ represent the terminal velocity in a Stokes flow regime and the characteristic sedimentation time of a single particle respectively. The Oseen velocity fields $\mathbf{v}^{\mathrm{O}}(\mathbf{x})$ which appear in Eq. (8) are calculated using Eq. (2).

2.3.2. Ordinary differential equation

The program developed in this work consists of integrating the differential equations arising from the NSL formulation, for each particle in its center of mass. Conventionally, these equations are written as:

$$\frac{\mathrm{d}\mathbf{s}}{\mathrm{d}t'} = \mathbf{g}(\mathbf{s}, t'), \quad \text{with } \mathbf{s}(t' = 0) = \mathbf{s}_0, \tag{14}$$

and where

$$\mathbf{s} = \begin{pmatrix} \mathbf{u} \\ \mathbf{x} \end{pmatrix}; \qquad \mathbf{g}(\mathbf{s}, t') = \begin{pmatrix} \mathbf{u}^0 + \mathbf{f} \\ \frac{\tau U_S}{a}\mathbf{u} \end{pmatrix}.$$

The set of equations is solved by applying Gear's method as an effective robust one. This is a predictor–corrector method with adaptative order and stepsize [16]. Eq. (14) is then numerically solved to obtain particle velocities and positions at any given time.

The development of the calculation algorithms is carried out in a Matlab environment which includes an appropriate solver for this kind of problem [17]. An equivalent tool is also developed in FORTRAN, to obtain more efficient calculations especially when a high number of particles interact.

3. Experimentations

3.1. Experimental apparatus

In our experiments, the suspending fluid is glycerine with a density of $1.25\,\mathrm{g\,cm^{-3}}$ and a viscosity $\mu = 0.85$ Pa s at a temperature $T = 22\ ^\circ\mathrm{C}$. The sedimenting particles are Teflon spheres with a diameter $2a = 6.35 \pm 0.05$ mm and a density of $2.15\,\mathrm{g\,cm^{-3}}$. Experiments have been carried out using a Plexiglass tank ($H = 1500$ mm), having a rectangular cross-section ($L = 100$ mm) $\times$ ($D = 500$ mm), which represents a ratio of confinement $(2a/L) = 6.35 \times 10^{-2}$. An experimental device has been especially set up to make sure that the particles are freed without any initial velocity. Particles are initially placed on stretched wires, with a distance of 5 mm between each one. An external mechanism fixed to each end ensures that the wires are symmetrically pushed back from the spheres, in order to free them. The main objective of this system is to have a low volume immersed in the suspending liquid and thereby it minimises hydrodynamic interactions between the particles and the device. In every case the temperature is measured after each series of experiments and the corresponding viscosity is determined using a pre-established calibration curve. A sketch of the experimental apparatus is shown in Fig. 1.

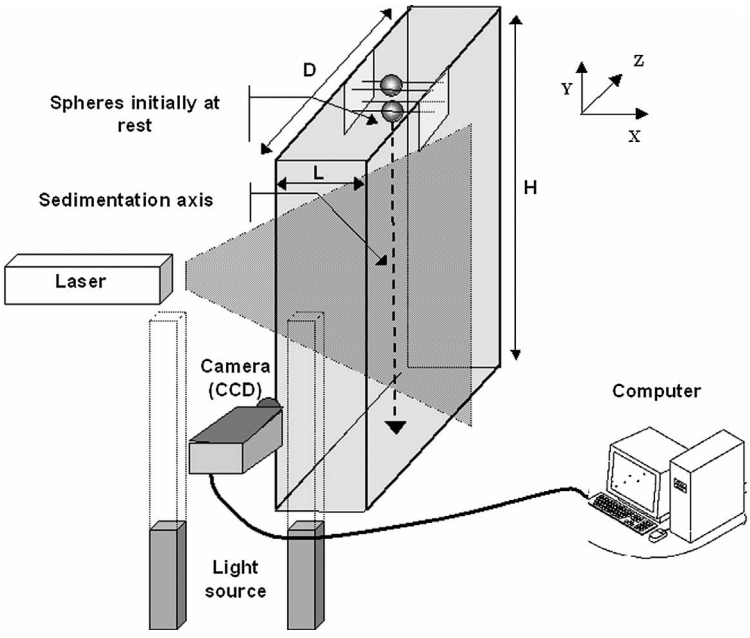

Fig. 1. Sketch of experimental apparatus.

Acquiring the particle positions is achieved by visualising them directly by means of a CCD camera (640 × 480), connected to a PC, with frontal lighting of the sedimentation field. The temporal measure sequence is controlled by software (Insight TSI). The particle trajectories are followed over a distance of up to 200 radius. On the experimental images a particle is represented by at least 6 × 6 pixels. The whole experiment consists in following the particle sedimentation in a vertical plane illuminated by a Laser sheet which ensures that the sedimentation takes place in this plane.

3.2. Image processing

A simple procedure of image processing is implemented in order to obtain satisfactory precision on the position of the center of each particle, for all of the images of a sequence. The bi-dimensional numerical signal making up each image is filtered using Fast Fourier Transforms. An image is generally a continuous function of the light intensity in zones separated by edges which present discontinuities. When the signal amplitude is increased to high frequencies (high-pass filter) the effect is to raise the edges but also the background noise of high frequencies. Consequently this high-pass filter technique is suitable to recognise the forms. On the opposite, if the amplitude of the high frequencies is lowered (low-pass filter), the contours are not as clear and the signal filtered in this way is continuous. This second technique enables the position of the centre of mass of the spherical particles to be determined. Moreover, it minimises the influence of the noise present on the experimental images. After filtering, a routine of barycentre calculation is automatically carried out, giving the position of the centre of mass of each particle with a precision of 0.15 pixel. However when particles are in close contact with each other, this technique is no longer applicable.

4. Results and discussions

Whatever the approach used to study the sedimentation of suspended particles and to validate the methodology used, the behaviour of an isolated sphere, a doublet, a triplet... must be successively considered. This is justified by the fact that the geometrical configuration and the flow conditions are the main parameters of the problem. This is why, in the following, we propose to successively consider configurations having one and then several particles.

First, the temporal evolution of velocity of an isolated sphere sedimenting in an infinite fluid may be obtained analytically in Stokes regime as well as in inertial regime. Our simulation results naturally confirm these predictions showing mainly the limit velocity at finite *Re* to be smaller than U_S. This shows simply that the numerical tool used is convenient to integrate the equations of motion.

When several particles interact under Stokes conditions, a typical configuration usually considered in literature is the sedimentation of three particles initially placed irregularly on a line in a horizontal plane perpendicular to the direction of gravity [14,1]. This case is taken up here to show on one hand that our numerical tool takes correctly into consideration the hydrodynamic interactions, and on the other hand to demonstrate that only slight differences are visible if sphere rotations are neglected.

For this purpose, three particles are initially placed horizontally ($y = 0$ and $x_1 = -5$; $x_2 = 0$; $x_3 = 7$) and their sedimentation is followed over a distance y of approximately 800 radius. The present simulation results are displayed in Fig. 2. The previous results obtained by Durlofsky et al. [1] under the same conditions are also shown in Fig. 2. It should be mentioned that the results of Durlofsky et al. [1] include sphere rotations. It can be seen in Fig. 2 that the results from our simulation and those including sphere rotations are consistent. This observation has been previously made by Ganatos et al. [14], who also noted that the contribution of the sphere rotations remains significantly low compared to their translations. Hence, large sedimentation distances must be reached before seeing them to play a significant role.

Whatever the case, the result from Fig. 2 clearly shows that the model used allows us to precisely describe the motion of hard spheres sedimenting in Stokes' flow regime. However, interactions between hard spheres sedimenting in inertial regime contrast with their behaviour under Stokes conditions. They exhibit some characteristic behaviours even at low Reynolds number. The simplest cases usually used to study these behaviours are configurations consisting of two spheres sedimenting along or perpendicular to their center-to-center vector **r**.

The case of the vertical doublet in sedimentation parallel to **r**, already dealt with from theoretical and experimental points of view, allows to provide quantitative data concerning the influence of the inertial effects on the dynamic behaviour of this doublet [18]. In this configuration, a decreasing of the gap between the particles is always observed, that means they move with different velocities. This phenomenon originate from the asymmetry of the Oseen velocity field and is naturally absent under Stokes conditions.

A simulation using our numerical tool, was carried out on a similar case. Two equal-sized spheres are placed vertically beside each other, with a predetermined distance r. Then the sedimentation is simulated over a sufficiently large distance and the instantaneous velocity of each particle is calculated. The ratio of the dimensionless velocity difference ($\Delta U/U_S = \Delta U^*$) to the Reynolds number obtained in the present study, is plotted versus the dimensionless center-to-center distance r/a in Fig. 3, for different values of *Re*. The reference Reynolds number used in Fig. 3 is calculated using the velocity U_S. It can

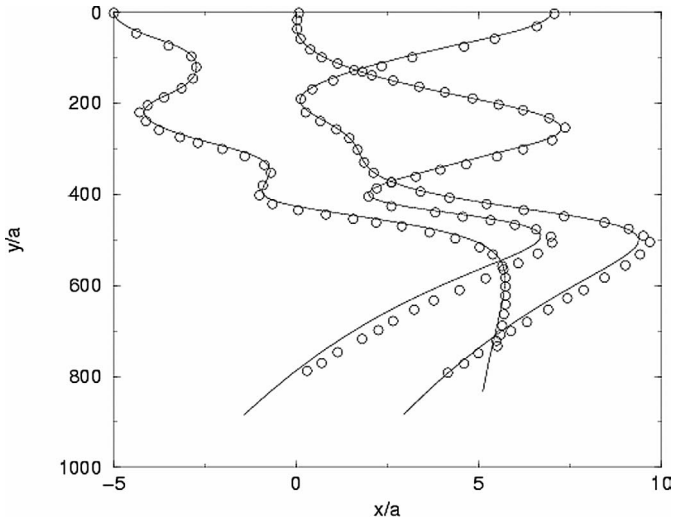

Fig. 2. Trajectories of three sedimenting particles ($Re = 0$). ($\circ\circ\circ$) represents the Durlofsky et al. result (numerised points) and (——) the numerical result.

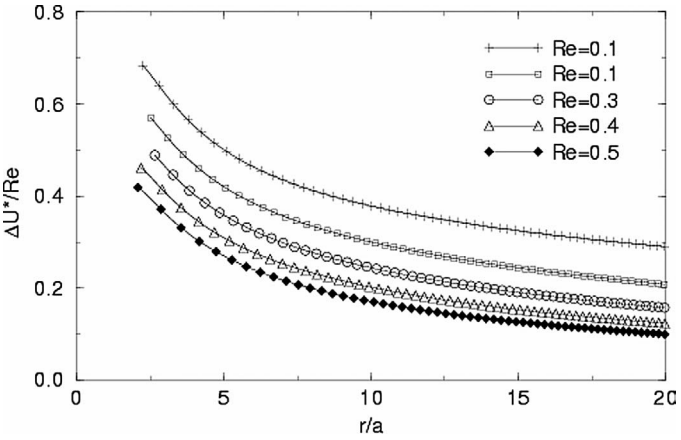

Fig. 3. Motion of two spheres initially located in a vertical plane. The ratio of velocity difference to the Reynolds number ($\Delta U^*/Re$) is plotted versus the center-to-center distance r.

be noticed that, for a given value of Re, the velocity difference increases when r decreases. At fixed separation distances this difference is an increasing function of the Reynolds number. That is to say, particles come quicker together at higher Re. The model proposed here seems to capture the physics of the problem. Moreover, according to literature, when the distance r is not too large and for low Reynolds numbers, the dimensionless velocity difference ΔU^* must be proportional to Re and the proportionality coefficient is $\frac{3}{8}$. Our simulations show however, that the proportionality coefficient is a function of the distance r. More precisely, if different Reynolds numbers are considered, distance r, for which the proportionality coefficient is $\frac{3}{8}$, verifies approximately $Re\frac{r}{a} \simeq 1$. This means that for a given range of Reynolds numbers and a given range of separation distances, the simulation results agreed with the theoretical relation $\Delta U^* = \frac{3}{8}Re$. Thus, for Re between 0.1 and 0.5, the validity of this relation is obtained for separation distances between 3 and 10 radius.

In the past, Happel et al. [18] carried out experiments in the same configuration. Their selected range of center-to-center distances is conform with the range given above. The velocity difference ΔU was measured for different values of the Reynolds number ($Re \leqslant 0.75$). They observed that, although the expected linearity is observed, the proportionality coefficient is lower than its theoretical value $\frac{3}{8}$. In order to correct this over-estimation of the inertial effects, these authors proposed to use an empirical coefficient $C_2 = 0.11$ rather than the predicted one. By this way, their experimental results were correctly reproduced over the whole investigated range of Reynolds numbers. Moreover, they notice that this coefficient is in fact almost twice the actual coefficient $C_1 = 0.05$, that should replace the theoretical coefficient $\frac{3}{16}$ in Eq. (3), in order to ensure the equality of the

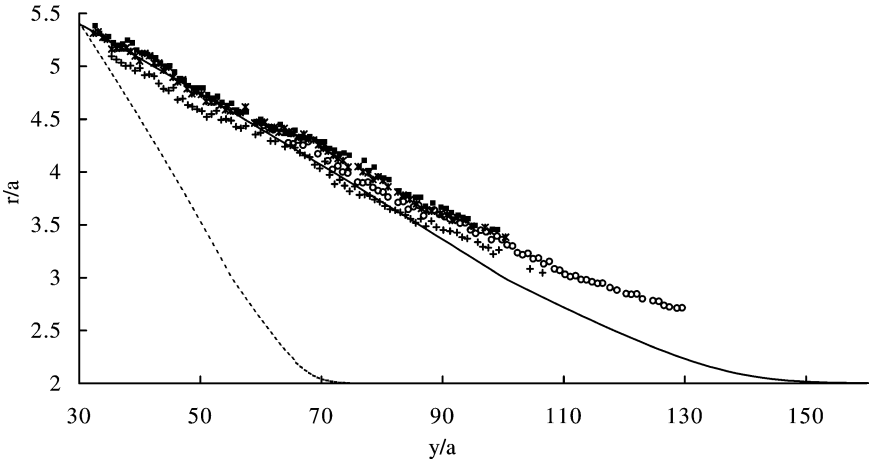

Fig. 4. Motion of two spheres initially located in a vertical plane ($Re = 0.3$). The center-to-center distance r versus the sedimentation distance y. Symbols represent experimental results, (——) the numerical result with C_1 and (– – –) the same result without C_1.

theoretical and experimental terminal velocity of an isolated sphere sedimenting in inertial regime. As far as we are concerned, we carried out sedimentation experiments of a vertical doublet for a Reynolds number $Re = 0.3$, using the experimental apparatus and the procedure as described in Section 3. This experiment was repeated several times and under the same experimental conditions. We were thus able to measure the particle positions with sufficient accuracy. Unfortunately, the range of velocity differences do not allow us to precisely determine ΔU. Nevertheless, with the trajectories obtained, we were still able to quite precisely represent the evolution of the distance r versus the sedimentation distance of the leading sphere; y_1. These results are displayed in Fig. 4 and show that when the spheres are not too close, the distance r seems to decrease linearly with the sedimentation distance y_1. On the opposite, as r approach a value of $4a$, the linearity is broken and the results seem to indicate, as expected, that a horizontal asymptote exists for the very low center-to-center distances and that the particles tend to sediment jointly.

The results of the numerical simulation represented by a dotted line in Fig. 4 also indicate an over-estimation of the inertial effects. However, when the coefficient C_1 proposed by Happel et al. [18] is introduced into the model at the individual particle level (Eqs. (2), (8)), good agreement can be observed between experimental results and numerical ones, at least in the linear zone. For formation of solid doublet, marked differences can be noticed between simulation and experimental data. It should be noticed that, in simulations, the Oseen velocity field given by Eq. (2) is used for all values of the distance between the spheres. The discrepancies observed may be attributed to the fact that, in the neighbourhood of the sphere, the non-linear term $(\mathbf{v} \cdot \nabla)\mathbf{v}$ which is in the complete momentum equation is of the same order as $(\mathbf{U} \cdot \nabla)\mathbf{v}$. This non-linear term should be taken into account to more precisely describe inertial effects in the inner region [11]. This is why our model should fall in describing hydrodynamic interactions between spheres at low separation distances, where the method of matched asymptotic expansions are more efficient [11].

It objectively raises the question if such correction is fortuitous and thereby restricted to the case considered, or if it can be generalised to all configurations, whatever the number of particles.

Let us consider now the sedimentation of two particles perpendicular to the vector $\mathbf{r}$. For that purpose, experiments were carried out on a horizontal doublet in sedimentation for a Reynolds number of 0.18, and the particle positions determined during the process. The experiment was again repeated several times and the distance r was measured during sedimentation. The obtained results are shown in Fig. 5. As expected, the inertial effects are manifested by a progressive spacing out of the particles as the sedimentation progresses. For the given Reynolds number, the distance r is a linear function of the sedimentation distance of the doublet; y. As shown in Fig. 4, it can be noticed that when the phenomenological correction proposed by Happel et al. [18] is not introduced, the simulation over-estimates, once again, the inertial effects (dotted-line curve). If the C_1 factor is taken into consideration as already described above, good agreement is then obtained between experimental results and the numerical ones.

We can therefore deduce that the numerical tool proposed provides a qualitative description of the interactions between particles in inertial regime at low Reynolds number. Quantitatively, introducing the C_1 factor makes our simulation tool able to reproduce the behaviour of a particle doublet, for all the considered configurations. Based on the above observations, the corrected model could be extended to study the sedimentation of a larger number of particles at low Reynolds numbers as far as separation distances between them are not too low.

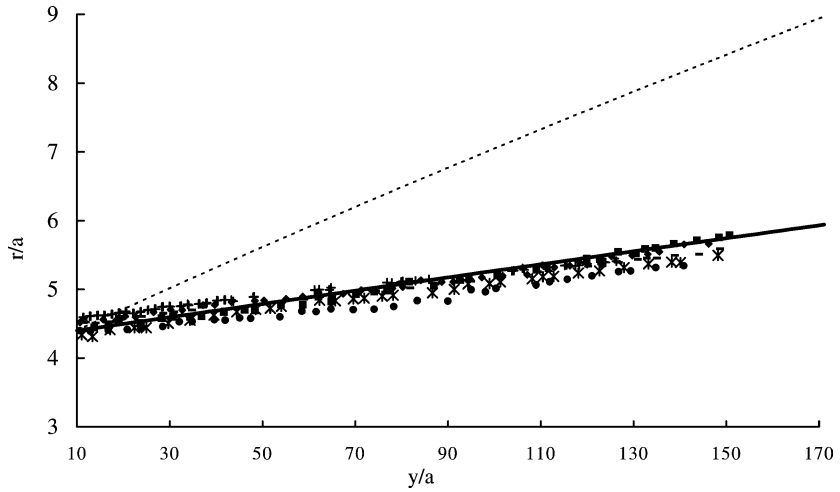

Fig. 5. Motion of two spheres initially located in a horizontal plane, perpendicular to the direction of gravity ($Re = 0.18$). The center-to-center distance r versus the sedimentation distance y. Symbols represent experimental results, (——) the numerical result with C_1 and (– – –) the same result without C_1.

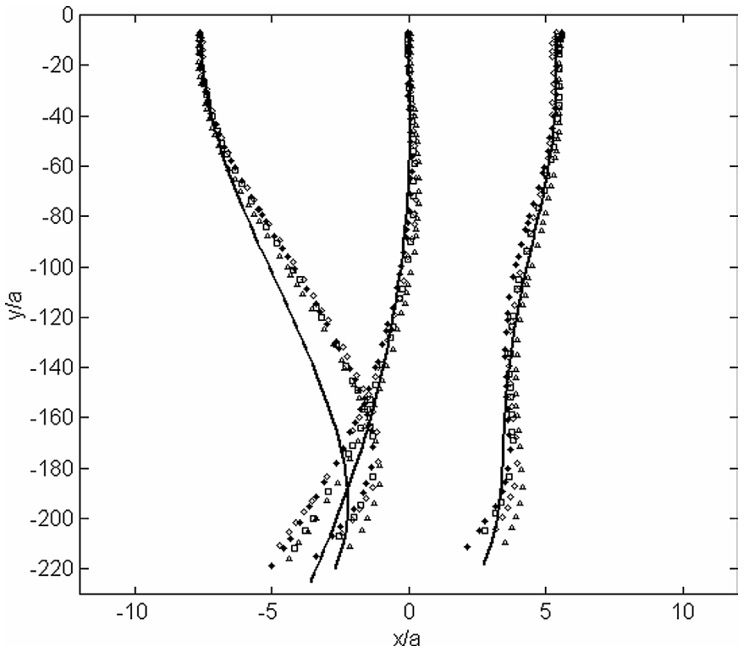

Fig. 6. Trajectories of three sedimenting particles initially located in a horizontal plane, perpendicular to the direction of gravity ($Re = 0.25$). Symbols represent experimental results, (——) the numerical result with C_1.

A logical follow-up to the hitherto discussed work is to study the sedimentation of a triplet of particles. A configuration similar to the one presented on Fig. 2 is considered but at finite *Re* and for the following initial positions: $x_1 = -7.72a$, $y_1 = 0$; $x_2 = 0$, $y_2 = -a$; $x_3 = 5.37a$, $y_3 = -0.7a$. Experiments are carried out and repeated several times for a Reynolds number of 0.25. The individual trajectories of the spheres are determined and displayed on Fig. 6, where the simulation results with the corrective factor C_1 included, are also shown. It can be noticed that the numerical simulation closely reproduces the pattern observed experimentally. It should be mentioned that when the corrective factor is not introduced, the numerical results diverge considerably from the experimental results and there is no crossing of the trajectories. Quantitatively, there are very low differences in the X direction and they remain comparable to the characteristic dimension of experimental differences, arising from the sensitivity to the initial conditions. In the Y direction, a higher divergence can be noted. Such divergence may be firstly

due to the same reasons as those invoked above to explain discrepancies between simulation predictions and experimental data, at low separation distances observed in the case of a vertical doublet.

An other explanation comes from wall effects. If we could consider that these effects are negligible when the ratio $(2a/L)$ is small and when the distance between the center of particles and walls are large compared to distances between particles (cases of doublets), it may be different in the present case. Initially the distance between the left wall and the center of particle 1 is less than $8a$ and is of the same order as the distance between spheres 1 and 2. If wall effects tend to decrease the sedimentation velocity of sphere 1 relative to sphere 2, we can expect that the sphere 1 will be attracted more quickly in the wake of sphere 2. This could explain why the crossing of trajectories occurs earlier in experiments.

Whatever the case, the numerical tool developed, including the C_1 corrective factor, once again demonstrates its ability to describe the behaviour of particles interacting in inertial regime. It was also successfully tested for higher numbers of particles in various configurations (preliminary results, to be published), with only a slightly higher calculation time.

5. Conclusions

In the present paper, we have studied both numerically and experimentally the sedimentation of several spheres at low Reynolds numbers. In the modelling part, the multi-body hydrodynamic forces were obtained after inversion of the two-body mobility matrix. Such mobility matrix was obtained by separating the velocity field generated by each particles in a Stokes-like part and a net inertial contribution and hypothesising that the first Faxen law is still applicable within a small error. The model hence developed shows its ability to predict particles sedimentation behaviour in Stokes flow regime as well as in weak inertial regime, at least qualitatively. However, the comparison of numerical and experimental data shows clearly the developed model to overestimate inertial effects. On contrary, if a corrective factor is introduced at the level of individual sphere, as done before by other authors, agreement between simulation results and experimental data is very satisfying whatever the configuration studied. So it is expected that, when the corrective factor is included, our model is able to predict sedimentation of more numerous spheres in various configurations as long as wall effects may be ignored.

References

[1] L. Durlofsky, J.F. Brady, G. Bossis, Dynamic simulation of hydrodynamically interacting particles, J. Fluid Mech. 180 (1987) 21–49.
[2] R.R. Bilodeau, D.W. Bousfield, Shear-thinning predictions from particle motion modeling, J. Rheology 42 (1998) 743–764.
[3] T. Kumagai, Numerical analysis of equation of motion for a cluster of spheres in fluid at low Reynolds number, JSME J. Ser. B 38 (4) (1995) 563–569.
[4] F. Feuillebois, Sedimentation in a dispersion with vertical inhomogeneities, J. Fluid Mech. 139 (1984) 145–171.
[5] A.B. Glendinning, W.B. Russel, A pairwise additive description of sedimentation and diffusion in concentrated suspension of hard spheres, J. Colloid. Interface Sci. 89 (1982) 124–143.
[6] W.B. Russel, D.A. Saville, W.R. Schowalter, Colloidal Dispersions, Cambridge University Press, 1995. First published 1989.
[7] J. Happel, H. Brenner, Low Reynolds Number Hydrodynamics, Prentice-Hall, 1965.
[8] D.J. Jeffrey, Y. Onishi, Calculation of the resistance and mobility functions for two unequal rigid spheres in low-Reynolds-number flow, J. Fluid Mech. 139 (1984) 261–290.
[9] D.J. Jeffrey, Y. Onishi, The forces and couples acting on two nearly touching spheres in low-Reynolds-number flow, J. Appl. Math. Phys. 35 (1984) 634–641.
[10] J.J. Gray, R.T. Bonnecaze, Rheology and dynamics of sheared arrays of colloidal particles, J. Rheology 42 (5) (1998) 1121–1151.
[11] P. Vasseur, R.G. Cox, The lateral migration of spherical particles sedimenting in a stagnant bounded fluid, J. Fluid Mech. 80 (1977) 561–591.
[12] P.G. Saffman, The lift on a small sphere in a slow shear flow, J. Fluid Mech. 22 (2) (1965) 385–400.
[13] G.K. Batchelor, An Introduction to Fluid Dynamics, Cambridge University Press, 1967.
[14] P. Ganatos, R. Pfeffer, S. Weinbaum, A numerical solution technique for three-dimensional Stokes flows with application to the motion of strongly interacting spheres in plane, J. Fluid Mech. 84 (1978) 79–111.
[15] N. Mordant, J.F. Pinton, Velocity measurement of a settling sphere, Eur. Phys. J. B 18 (2000) 343–352.
[16] C.W. Gear, L.R. Petzold, ODE methods for the solution of differential algebric systems, J. Numer. Anal. 21 (4) (1984).
[17] L.F. Shampine, M.W. Reichelt, The MATLAB ODE suite, SIAM J. Sci. Comput. 18-1 (1997).
[18] J. Happel, R. Pfeffer, The motion of two spheres following each other in a viscous fluid, AIChE J. 6 (1) (1960) 129–133.